

Gaia luminosities of pulsating A-F stars in the Kepler field

L. A. Balona

South African Astronomical Observatory, P.O. Box 9, Observatory, Cape 2735, South Africa

Accepted Received ...

ABSTRACT

All stars in the *Kepler* field brighter than 12.5 magnitude have been classified according to variability type. A catalogue of δ Scuti and γ Doradus stars is presented. The problem of low frequencies in δ Sct stars, which occurs in over 98 percent of these stars, is discussed. Gaia DR2 parallaxes were used to obtain precise luminosities, enabling the instability strips of the two classes of variable to be precisely defined. Surprisingly, it turns out that the instability region of the γ Dor stars is entirely within the δ Sct instability strip. Thus γ Dor stars should not be considered a separate class of variable. The observed red and blue edges of the instability strip do not agree with recent model calculations. Stellar pulsation occurs in less than half of the stars in the instability region and arguments are presented to show that this cannot be explained by assuming pulsation at a level too low to be detected. Precise Gaia DR2 luminosities of high-amplitude δ Sct stars (HADS) show that most of these are normal δ Sct stars and not transition objects. It is argued that current ideas on A star envelopes need to be revised.

Key words: stars: oscillations - stars: variables: δ Scuti - parallaxes

1 INTRODUCTION

The δ Sct stars are A and early F dwarfs and giants with multiple frequencies in the range $5\text{--}50\text{ d}^{-1}$ while γ Dor stars are F dwarfs and giants pulsating in multiple frequencies in the range $0.3\text{--}3\text{ d}^{-1}$. The two types of variable have been considered as two separate classes of pulsating star driven by different mechanisms: the opacity-driven κ mechanism in δ Sct stars and the convective blocking mechanism in γ Dor stars as described by Guzik et al. (2000).

Simultaneous low-frequency γ Dor and high-frequency δ Sct pulsations in the same star were first discovered by Handler et al. (2002) in the A9/F0V star HD 209295. Until then none of the hundreds of known δ Sct stars were found to contain low frequencies. The discovery was at variance with the predictions of models using the κ mechanism in which frequencies below 5 d^{-1} are stable.

Before the advent of the *CoRoT* and *Kepler* missions, only six δ Sct/ γ Dor hybrids had been discovered. They all lie roughly at the high-temperature end of the known γ Dor instability strip, but extending beyond the strip to higher temperatures. With the first release of the *Kepler* data, it became clear that the hybrids were not rare at all (Grigahcène et al. 2010). From only 50 days of data, at least one-quarter of δ Sct stars were found to be hybrids. In this paper it is found that significant low-frequency peaks are present in at least 98 percent of stars. Hybrid behaviour is the norm and occurs even among the hottest stars, as shown by Balona et al. (2015).

The reason why so few hybrids were discovered from the ground must be partly attributed to the fact that ground-based photometry is greatly affected by variations in atmospheric extinction and daily data gaps, masking the low amplitudes of the long-period pulsations. The few hybrids discovered from the ground appear to be located in the region of instability where largest amplitudes tend to occur (Balona 2014).

Recent pulsation models using time-dependent perturbation theory show that there is a complex interplay of driving and damping processes which cannot be reduced to just the κ or convective blocking mechanisms. Xiong et al. (2015) and Xiong et al. (2016) show that factors such as turbulent dissipation, turbulent diffusion and anisotropy of turbulent convection need to be considered. Furthermore, in a region with a radiative flux gradient, the flux will itself be modulated by the oscillations. This is called “radiative modulation excitation” (RME) by Xiong et al. (1998). These additional factors co-exist and appear to explain the low frequencies seen in these stars. As Xiong et al. (2016) point out, from this point of view both δ Sct and γ Dor stars may be regarded as a single class of pulsating variable.

High-precision *Kepler* photometry has enabled a large number of pulsating variables to be detected in the *Kepler* field. In this paper a list of δ Sct and γ Dor stars, complete to *Kepler* magnitude $K_p = 12.5\text{ mag}$ but including fainter stars, is presented. Using photometric or spectroscopic estimates of effective temperature and luminosities determined from the parallaxes in the second data release of Gaia (Gaia

DR2; [Gaia Collaboration et al. 2018](#)), these stars are precisely located in the Hertzsprung-Russell (H-R) diagram. Comparison between the observed and calculated red and blue edges are made. In addition to the problem of low frequencies in δ Sct stars, it is shown that less than half the stars in the instability strip pulsate. It is argued that this cannot be a result of pulsations at a level too low to be detected. Finally, it is shown that most of the high-amplitude δ Sct stars (HADS) are normal δ Sct stars and not objects intermediate between δ Sct and Cepheid variables.

2 THE PROBLEM OF THE LOW FREQUENCIES

Models using the κ mechanism show pulsational instability in main sequence and giant stars of intermediate mass only for frequencies higher than about 5 d^{-1} . Lower frequencies are all stable. It may be possible to account for low frequencies as a result of rotational splitting. One can introduce rotational splitting in a simple way by using the known distribution of equatorial velocities among A/F dwarfs and giants using frequencies obtained from non-rotating models. The frequency distributions obtained in this way can be compared to observations, but they do not agree with the observed distributions ([Balona et al. 2015](#)). It seems that low frequencies cannot be explained as a result of rotation.

It is also possible that inertial modes, in particular r modes ([Papaloizou & Pringle 1978](#)), might account for the low frequencies. These modes consist of predominantly toroidal motions which do not cause compression or expansion and hence no light variations. However, in a rotating star, the toroidal motion couples with spheroidal motion caused by the Coriolis force, leading to temperature perturbations and hence light variations. These modes have been recently proposed as an explanation of the broad hump that appears just below the rotation frequency in many A stars and also period spacings in some γ Dor stars ([Saio et al. 2018](#)).

If r modes are responsible for the low frequencies in δ Sct stars, then all rotating stars within the instability strip should show such frequencies. This is not the case; in fact the majority of stars in the δ Sct instability strip do not seem to pulsate at all. For this reason, inertial modes can be ruled out as the cause of the low frequencies in δ Sct stars.

[Balona et al. \(2015\)](#) examined the possibility that the opacities in the outer layers of A stars may be underestimated. Artificially increasing the opacities by a factor of two does lead to instability of some low-degree modes at low frequencies, but also decreases the frequency range of δ Sct pulsations to some extent. An increase in opacities by such a large factor is unlikely and at present cannot be regarded as a possible solution to this problem.

A fundamental obstacle to our understanding of stellar pulsations is that we lack a suitable theory of convection. The treatment of convection in pulsating stars has progressed quite considerably since the description of the γ Dor pulsation mechanism in terms of “convective blocking” ([Guzik et al. 2000](#)). Convective blocking uses the simplest description of convection and does not take into account the interaction between pulsation and convection. Such “frozen-in” convection precludes the possibility of predicting the red

edge of the δ Sct and γ Dor instability strips. More recent treatments of pulsation use time-dependent perturbation theory ([Dupret et al. 2005a,b](#)). This allows the interaction between pulsation and other processes, such as turbulent pressure and turbulent kinetic energy dissipation, to be included.

According to the time-dependent convection model of [Houdek \(2000\)](#), the damping of pulsations at the red edge of the δ Sct instability strip appears to be mostly due to fluctuations of the turbulent pressure which oscillates out of phase with the density fluctuations. However, in the models of [Xiong \(1989\)](#) and [Dupret et al. \(2005a\)](#), turbulent pressure driving and turbulent kinetic energy dissipation damping cancel near the red edge and stability is determined by the perturbations of the convective heat flux. All models are able to predict the red edge, but further research is necessary to identify the correct processes. A more detailed discussion can be found in [Houdek & Dupret \(2015\)](#).

Existing theories of convection rely on unknown parameters to characterize the effects of turbulent pressure and turbulent kinetic energy dissipation. The parameters are adjusted to obtain best agreement with observations. For example, three parameters are introduced by [Xiong et al. \(2015\)](#). In order to fix these parameters the observed red and blue edges of the δ Sct and γ Dor instability strips need to be determined. At present these are poorly known due to the large error in the luminosities. This problem can now be solved using distances derived from Gaia DR2 parallaxes ([Gaia Collaboration et al. 2016](#)).

3 THE DATA

The *Kepler* observations consist of almost continuous photometry of many thousands of stars over a four-year period. The vast majority of stars were observed in long-cadence (LC) mode with exposure times of about 30 min. *Kepler* light curves are available as uncorrected simple aperture photometry (SAP) and with pre-search data conditioning (PDC) in which instrumental effects are removed ([Stumpe et al. 2012](#); [Smith et al. 2012](#)). Most stars in the *Kepler* field have been observed by multicolour photometry, from which effective temperatures, surface gravities, metal abundances and stellar radii can be estimated. These stellar parameters are listed in the *Kepler Input Catalogue* (KIC, [Brown et al. 2011](#)).

Subsequently, [Pinsonneault et al. \(2012\)](#) and [Huber et al. \(2014\)](#) revised these parameters for stars with $T_{\text{eff}} < 6500 \text{ K}$. For hotter stars, the KIC effective temperatures were compared with those determined from high-dispersion spectroscopy by [Balona et al. \(2015\)](#). It was found that the KIC temperatures are very well correlated with the spectroscopic temperatures, but 144 K cooler. Adding 144 K to the KIC temperatures reproduces the spectroscopic temperatures with a standard deviation of about 250 K. This can be taken as a realistic estimate of the true standard deviation since the KIC and spectroscopic effective temperatures are independently determined. In this paper the values of T_{eff} given by [Huber et al. \(2014\)](#) are used for stars with $T_{\text{eff}} < 6500 \text{ K}$. For hotter stars, the KIC effective temperatures, increased by 144 K, are used.

To determine the luminosities of *Kepler* δ Sct and γ Dor stars requires knowledge of the apparent magnitude, inter-

stellar extinction, bolometric correction and the parallax. A table of the bolometric correction, BC, in the Sloan photometric system as a function of T_{eff} and $\log g$ is presented in [Castelli & Kurucz \(2003\)](#). For this purpose, the small corrections described by ([Pinsonneault et al. 2012](#)) are applied to the *Kepler* *griz* magnitudes to bring them into agreement with the Sloan system. Correction for interstellar extinction was applied to the *r* magnitude using $r_0 = r - 0.874A_V$ ([Pinsonneault et al. 2012](#)).

The value of A_V listed in the KIC is from a simple reddening model which depends only on galactic latitude and distance. A three-dimensional reddening map with a radius of 1200 pc around the Sun and within 600 pc of the galactic midplane has been calculated by [Gontcharov \(2017\)](#). This is likely to produce more accurate values of A_V and is used in this paper. For more distant stars, the simple reddening model is used but adjusted so that it agrees with the 3D map at 1200 pc. A comparison shows that the KIC values of A_V are typically 0.017 mag higher than those given by the 3D map.

From the Gaia DR2 parallax, π , the absolute magnitude is calculated using $r_{\text{abs}} = r_0 + 5(\log_{10} \pi + 1)$. The absolute bolometric magnitude is then given by $M_{\text{bol}} = r_{\text{abs}} + \text{BC}_r - M_{\text{bol}\odot}$ with the solar absolute bolometric magnitude $M_{\text{bol}\odot} = 4.74$. Finally, the luminosity relative to the Sun is found using $\log L/L_{\odot} = -0.4M_{\text{bol}}$.

4 CLASSIFICATION AND LIGHT CURVES

Stars in the *Kepler* field were observed almost continuously for 17 quarters covering a period of just over 4 years. Light curves and periodograms of all short-cadence observations (4827 stars) were visually examined. All long-cadence data brighter than magnitude 12.5, but including many more stars fainter than this limit (20784 stars in total) were visually examined as well.

Detection of δ Sct stars is relatively easy since the periodograms show peaks at high frequencies. The β Cep variables and some types of compact stars also show high frequencies, but these can be distinguished from δ Sct using the KIC effective temperatures and surface gravities. Among the 20784 stars examined, 1740 δ Sct stars were discovered.

The distinction between δ Sct and γ Dor stars was based purely on the absence of peaks with significant amplitudes having frequencies in excess of around 5 d^{-1} . These stars have multiple peaks below this frequency.

It is sometimes difficult to distinguish between γ Dor and rotating variables which are the very common. Classification as a γ Dor star was made only if the frequencies were too widely spread to be due to differential rotation. It should be noted that surface differential rotation reaches a maximum in the F stars ([Balona & Abedigamba 2016](#)) where most γ Dor stars are to be found. It is possible that at least some frequency peaks in γ Dor stars may be due to rotation. γ Dor stars are distinguished from the slowly pulsating B (SPB) stars and some compact objects using the KIC effective temperatures and surface gravities. Among the 20784 stars examined, 820 γ Dor stars were discovered.

During the course of examination of the periodograms, instances were noted of the presence of low-frequency peaks in δ Sct stars, excluding peaks which might be attributed to

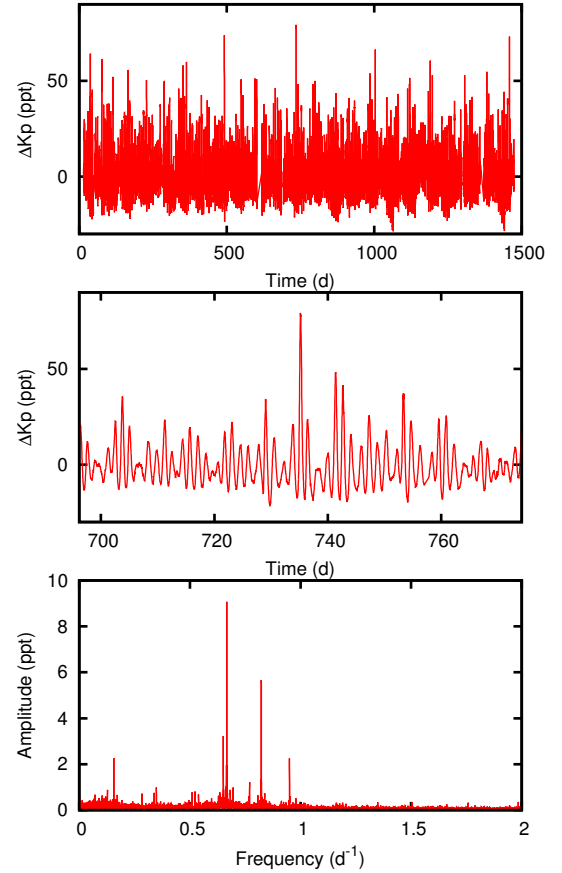


Figure 1. Top panels: *Kepler* light curve of KIC 8180361 showing asymmetrical light curve with occasional large excursions, one of which is depicted in the middle panel. The periodogram is shown in the bottom panel.

binarity or rotation. The number of stars without significant low frequencies was found to be very low, probably less than 2 percent of the δ Sct stars. Thus nearly all δ Sct stars are hybrids.

Even a cursory examination of the *Kepler* light curves reveals a set of stars with beating and highly asymmetric minima and maxima. Maximum light amplitudes far exceeded those of minimum light. In many cases sudden high-amplitude excursions can easily be mistaken for flares. The morphology of these light curves is striking and quite unlike any other type of variable. These γ Dor stars were first described by [Balona et al. \(2011\)](#) who named them the ASYM (asymmetric) type of γ Dor variable.

Fig. 1 shows an example of the light curve and periodogram of the ASYM type. It should be noted that the *Kepler* PDC light curve flags most of the flare-like excursions as bad points. The light curve shown in the figure was reconstructed from the raw data using the good points of the PDC data to determine the necessary corrections. One of the questions that need to be asked is whether the large excursions arise as a result of beating of sinusoidal components. This can be answered by clipping the light curve to eliminate the large excursions. If the sudden high maxima are a simple result of beating of pure sinusoids, clipping these maxima should not introduce new frequencies. The periodogram of the clipped data shows significantly fewer low-

Table 1. An extract of the δ Sct and γ Dor catalogue in the *Kepler* field. The full table is available in electronic form. The first two columns is the KIC number and the type of variable. The Gaia DR2 parallax (Plx) and its standard deviation (ePlx) are in milliarcseconds. The effective temperature and its error are in K. The interstellar absorption, A_V (mag) is derived from the tables in [Gontcharov \(2017\)](#). Finally, the relative solar luminosity and its error is given.

KIC	Type	Plx	ePlx	T_{eff}	e T_{eff}	A_V	$\log L/L_\odot$	e $\log L/L_\odot$
1026294	DSCT	1.0562	0.0245	8083	280	0.38	1.2026	0.042
1161908	GDORS	0.8361	0.0141	6662	198	0.45	0.8021	0.041
1162150	DSCT	0.9272	0.0247	7015	263	0.46	1.6332	0.042
1163943	DSCT	1.2370	0.0317	7236	241	0.33	1.2845	0.042
1294670	DSCT	0.5840	0.0254	7220	276	0.53	1.6572	0.044
1430590	DSCT	0.8833	0.0278	6899	253	0.48	1.0904	0.042
1430741	GDORM	0.4982	0.0171	7091	277	0.53	1.1261	0.043
1431379	GDORS	1.0646	0.0242	7106	245	0.39	0.9482	0.042
1431794	DSCT/ROT	0.8712	0.0234	7255	273	0.46	1.2349	0.042

Table 2. An extract of the catalogue of δ Sct and γ Dor stars in the *Kepler* field for which Gaia DR2 luminosities could not be obtained. The *Kepler* magnitude, K_p , the effective temperature, T_{eff} , and its error and the luminosity, $\log L/L_\odot$, determined from T_{eff} and the KIC radii are given. The error in $\log(L/L_\odot)$ is about 0.4 dex.

KIC	Type	K_p	T_{eff}	e T_{eff}	$\log L/L_\odot$
1571152	DSCT	9.268	7192	149	1.88
2568519	GDORS	11.258	6299	182	0.18
2572386	DSCT	13.278	7345	275	
2856756	DSCT	10.250	10477	365	2.39
2975832	DSCT	12.610	6824	249	

amplitude peaks, indicating that these additional frequency components are required and that the excursions are simply due to a highly non-linear physical process.

The light curves of most γ Dor stars show characteristic beating, but with symmetric minima and maxima (the SYM type). The beating may be traced to two or more dominant closely-spaced frequencies in the periodograms. Another type of γ Dor star shows no obvious beating in the light curve and an even frequency spread of peaks in the periodogram with comparable amplitudes (the MULT type). Because the distinction between the three groups may be important, each star was classified as either GDORA, GDORS or GDORM corresponding to the ASYM, SYM and MULT types.

Among the 820 γ Dor stars there are 137 GDORA and 447 GDORS stars. There are 16 stars which are GDORS for some of the time and GDORA at other times. There are 215 GDORM stars. A few stars which are difficult to classify into the three groups are labeled simply as GDOR.

A catalogue of the δ Sct and γ Dor stars is available in electronic form. An extract from the catalogue is shown in Table 1. In this table the effective temperatures for $T_{\text{eff}} < 6500$ K are from [Huber et al. \(2014\)](#). For hotter stars, 144 K has been added to the KIC effective temperature as discussed above. The interstellar absorption, A_V , is obtained from the 3D map of [Gontcharov \(2017\)](#). If the KIC values of A_V are used, the higher absorption leads to a slight increase in $\log L/L_\odot$ of only 0.006 dex. There are 1680 δ Sct stars

and 796 γ Dor stars with luminosities estimated from Gaia DR2 parallaxes.

For some stars Gaia DR2 parallaxes do not exist, no effective temperature is available or the interstellar extinction cannot be estimated. These 94 stars are listed separately (see Table 2 for an extract).

The mean difference between the photometrically estimated luminosities, $\log(L/L_\odot)_P$, and the luminosities from Gaia DR2, $\log(L/L_\odot)_G$, is $< \log(L/L_\odot)_P - \log(L/L_\odot)_G > = -0.22 \pm 0.01$. The photometrically estimated luminosities have a standard error of 0.39 dex.

When deriving the location of the instability strips, the surface gravity, $\log g$, as a function of T_{eff} is sometimes used instead instead of $\log L/L_\odot$ as a function of T_{eff} (eg. [Uytterhoeven et al. 2011](#)). This is simply because $\log g$ can be directly obtained from the observations. However, for comparison with theoretical models, $\log L/L_\odot$ is to be preferred. In this paper, $\log L/L_\odot$ is the natural choice because it can be obtained directly from the parallax as described above. Moreover, the Gaia DR2 parallaxes result in luminosities with very high accuracy, so that the instability strip can be determined far more precisely than the use of $\log g$.

Many stars are binaries. If a star is a binary with components of equal luminosity, the luminosity calculated from the parallax will be twice as large as a single star of the same luminosity. Thus $\log L/L_\odot$ will be too high by about 0.3 dex. We do not know which stars are binaries in the *Kepler* field and it is possible that the estimated $\log L/L_\odot$ may be too large for some stars. If the components have different temperatures, this will also affect the T_{eff} of the combined stars. Unfortunately without detailed spectroscopic observations of each star it is impossible to correct for these effects.

5 THE δ SCT STARS

In Fig. 2 the δ Sct stars are shown in the H-R diagram together with the zero-age main sequence from models with solar abundances ($Z = 0.017$) and helium abundance $Y = 0.26$ by [Bertelli et al. \(2008\)](#). The dashed polygon is a visual estimate of the location of the majority of the δ Sct stars and includes 94 percent of these stars. Most of the stars are within the temperature range $6580 < T_{\text{eff}} < 9460$ K. The typical standard deviation is about 260 K in T_{eff} (0.015 in $\log T_{\text{eff}}$) and about 0.052 in $\log(L/L_\odot)$. These errors are shown by the cross in Fig. 2. The main uncertainty in the luminosities is the effect of interstellar light absorption. The extinction values used here are interpolated from the table by [Gontcharov \(2017\)](#). Reduced extinction will lead to smaller luminosities. Also shown in the figure are the red and blue edges from [Xiong et al. \(2016\)](#). The effective temperatures of the red and blue edges are clearly too cool.

There are a number of outliers on both the hot and cool sides of the instability region which need further study. It is possible that their effective temperatures are in error, but a study by [Balona et al. \(2016\)](#) suggests that there is evidence for a class of variables with multiple high frequencies characteristic of β Cep and δ Sct stars which lie between the red edge of the β Cep and the blue edge of the δ Sct instability regions. These have been called Maia variables. The few outliers below the ZAMS may be evolved objects, though the KIC surface gravities seem to be normal.

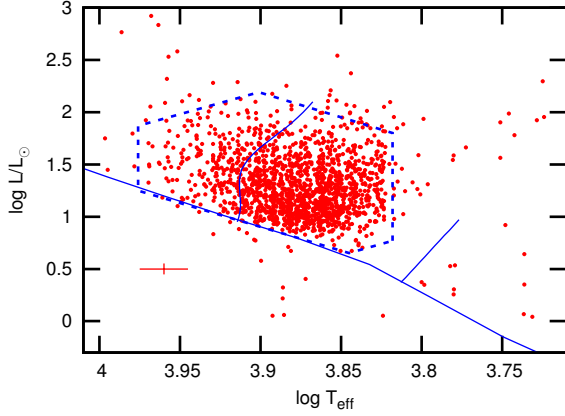


Figure 2. *Kepler* δ Sct stars in the H-R diagram (dots) using Gaia DR2 parallaxes and Gontcharov (2017) values of A_V . The solid lines are the zero-age main sequence (solar abundance from Bertelli et al. (2008)) and the nonradial red and blue edges from Xiong et al. (2016). The dashed polygon defines the region which includes the majority of δ Sct stars. The cross on the bottom left shows the $1\text{-}\sigma$ error bars.

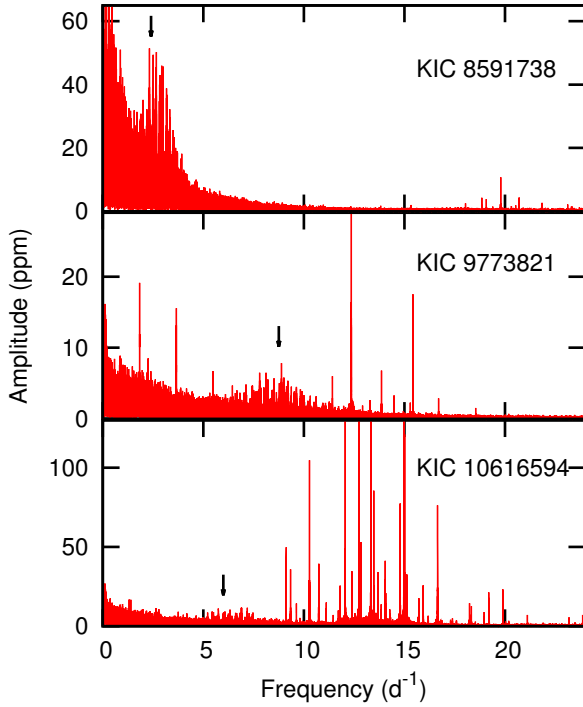


Figure 3. Examples of stars which show both solar-like oscillations (indicated by the arrow) and δ Sct high frequencies. These are composite stars containing a cool giant and a δ Sct star.

Qian et al. (2018) observed a group of 131 cool multi-periodic variable stars that are much cooler than the red edge of the δ Sct instability strip. Many of these are in the *Kepler* field. Inspection of their periodograms show the typical Gaussian amplitude envelope characteristic of solar-like oscillations, so it is possible that Qian et al. (2018) have misclassified solar-like pulsations in red giants as δ Sct stars. There is no indication of a cool population of δ Sct stars among the *Kepler* data examined. There are, however, com-

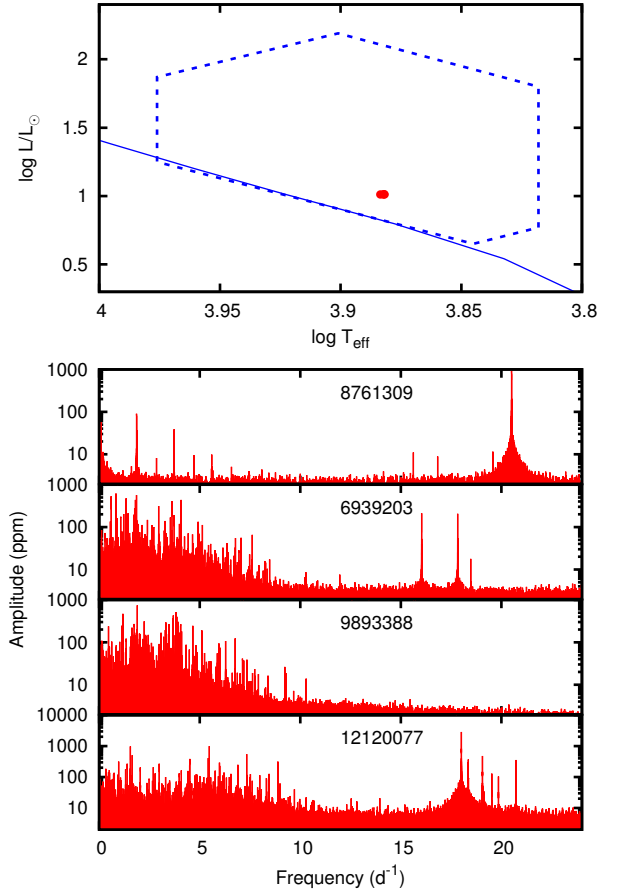


Figure 4. Example of periodograms of four δ Sct stars which have practically the same stellar parameters. The top panel shows their location in the H-R diagram, all within the single filled circle. The ZAMS and the δ Sct instability region are shown.

posite objects consisting of a cool giant and a normal δ Sct star. Fig. 3 shows periodograms of three of these stars where the Gaussian-like amplitude envelope characteristic of solar-like oscillations in a cool giant and the pulsations in a δ Sct star are clearly visible.

There are other cool stars that can be classified as δ Sct variables. An example is KIC 4142768 where the effective temperature from several sources (including the KIC) is only about 5400 K. The star is a heartbeat variable (Balona 2018) and the LAMOST spectrum is A9V with no sign of a cool giant. In this case the explanation may be additional reddening caused by gas and dust associated with the binary.

Fig. 4 is an illustration of the disparity in frequencies and amplitudes among δ Sct stars with practically the same stellar parameters. All four stars have $\log T_{\text{eff}} = 7630$ K and $\log L/L_{\odot} = 1.012$ within 20 K and 0.002 dex respectively. The disparity in the general appearance in frequency peaks is remarkable. It is possible that rotation may be an important factor or that some of the four stars may be composite which will affect the derived luminosity. Also, the observational error of around 250 K in T_{eff} could modify the expected pulsation frequencies somewhat. Nevertheless, the general impression obtained from visual inspection is that the periodogram of each star is unique.

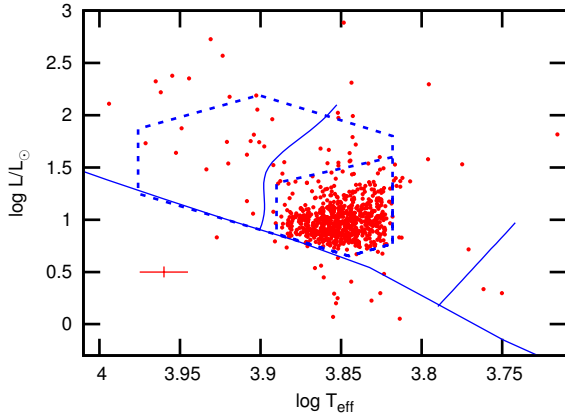


Figure 5. The location of the γ Dor stars in the H-R diagram (dots) using Gaia DR2 parallaxes and [Gontcharov \(2017\)](#) values of A_V . The outer dashed polygon defines the instability region of δ Sct stars. The smaller polygon defines the approximate location of γ Dor stars. The solid lines show the zero-age main sequence and the red and blue edges of the instability strip calculated by [Xiong et al. \(2016\)](#).

Table 3. Coordinates of the vertices of the δ Sct and γ Dor instability regions as shown in Figs. 2 and 5.

δ Sct		γ Dor	
$\log T_{\text{eff}}$	$\log L/L_{\odot}$	$\log T_{\text{eff}}$	$\log L/L_{\odot}$
3.818	0.770	3.818	1.600
3.818	1.800	3.890	1.350
3.901	2.190	3.890	0.867
3.976	1.870	3.845	0.651
3.976	1.250	3.818	0.770
3.845	0.651	3.818	1.400
3.818	0.770		

6 THE γ DOR STARS

In Fig. 5 the γ Dor stars are shown in the H-R diagram together with the zero-age main sequence from models with solar abundance ([Bertelli et al. 2008](#)). The figure shows the instability polygon of the δ Sct stars as reference. The smaller nested polygon contains 89 percent of the γ Dor stars. The coordinates of the vertices in the polygonal regions of the δ Sct and γ Dor stars are listed in Table 3.

As mentioned above, a star was classified as a γ Dor variable only if all the peaks in the periodogram are below 5 d^{-1} (with some leeway if there are a few peaks of low amplitude above this frequency). In addition, a very important qualification is added: the frequencies must exclude rotational modulation. If, for example, a peak and its harmonic is seen, then it is a rotational variable and not a γ Dor. It is this criterion more than anything else which is responsible for refining the γ Dor instability strip. Of course, the luminosities derived from Gaia DR2 also assist in this refinement. The location of δ Sct and γ Dor stars using KIC radii and effective temperatures to determine the luminosities is shown in Fig. 2 of [Balona \(2014\)](#). These can be compared with Fig. 2 and 5 in this paper.

It is interesting that the γ Dor instability region lies completely within the δ Sct instability region. In the γ Dor

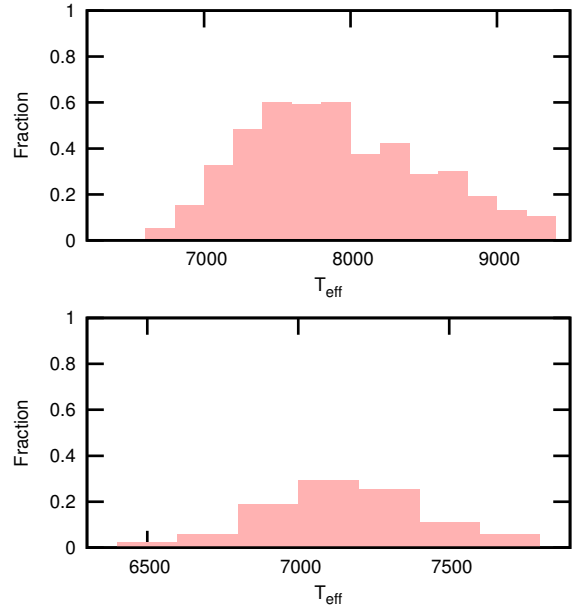


Figure 6. Top panel: the fraction of δ Sct stars in the instability box relative to all stars in the box as a function of effective temperature. Bottom panel: the fraction of γ Dor stars relative to all stars in the γ Dor box as a function of effective temperature.

box there are 711 γ Dor stars, but there are also 815 δ Sct stars (and 994 other objects) in the same box. It seems that the γ Dor variables are simply a subset of the δ Sct stars and not an independent class, as suggested by [Xiong et al. \(2016\)](#). There is no difference in the locations of the GDORA, GDORS and GDORM subtypes within the γ Dor box. The red and blue edges of the γ Dor instability strip calculated by [Xiong et al. \(2016\)](#) are shown in the figure, but do not agree with observations.

There are quite a number of hot outliers which have been studied by [Balona et al. \(2016\)](#). The spectra confirm that many of these stars are indeed hot γ Dor stars. Whether or not these deserve a separate classification or whether these stars, like the γ Dor stars, may just be due to unusual mode selection processes remains to be seen.

[Mowlavi et al. \(2013\)](#) found a large population of new variable stars between the red edge of the SPB stars and the blue edge of the δ Sct stars, a region in the H-R diagram where no pulsation is predicted to occur based on standard stellar models. Their periods range from 0.1–0.7 d, with amplitudes between 1 and 4 mmag. It is possible that these could be identified with the hot γ Dor stars in the *Kepler* field.

The three coolest γ Dor stars (KIC 4840401, 8264287, and 12218727) are not solar-like variables. No known variable class in this temperature range resembles the γ Dor class. They could be composite objects, but merit further study. The stars lying below the ZAMS also merit further study. They may perhaps be evolved compact objects.

7 FRACTION OF PULSATING STARS

In order to determine whether or not all stars in the δ Sct instability region pulsate, it is necessary to count the number

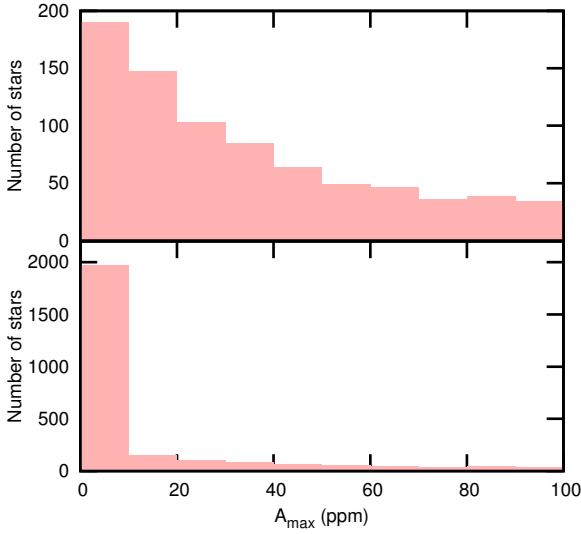


Figure 7. Top panel: the distribution of the maximum amplitude (ppm) in *Kepler* δ Sct stars with $K_p < 12.5$ mag in the instability box. Bottom panel: As above, but including all stars with $K_p < 12.5$ mag in the δ Sct instability box on the assumption that these “constant” stars actually pulsate at below the detection limit. The peak at $A_{\max} < 10$ ppm reaches 1781 stars.

of pulsating and non-pulsating stars within the same region. To assure completeness, the sample is limited to stars with $K_p < 12.5$ mag because all stars in the *Kepler* field down to this brightness level have been classified according to variability class.

It is found that 2881 stars for which luminosities can be determined from Gaia DR2 lie within the δ Sct instability box (excluding known evolved objects). Of these, 874 are δ Sct stars and 281 are γ Dor stars. The remainder are non-pulsating as far as can be ascertained. Most are rotational variables or eclipsing systems. There are 1759 stars within the γ Dor instability region, of which 260 are γ Dor stars and 401 are δ Sct stars.

The number of δ Sct stars relative to the total number of stars within the δ Sct instability box varies as a function of effective temperature (Fig. 6, top panel). The largest fraction of δ Sct stars occurs around $T_{\text{eff}} \approx 7600$ K. The bottom panel of the same figure shows the relative number of γ Dor stars in the γ Dor instability box as a function of temperature.

These results strongly indicate that both pulsating and non-pulsating stars co-exist within the instability strip. This poses a problem because it is difficult to understand why some stars with closely similar parameters, and with presumably very similar driving and damping regions, should pulsate while others do not pulsate. It is possible to argue that the non-pulsating stars do pulsate, but at a level below the detection limit, but statistics of the amplitude distribution argue against this (Balona & Dziembowski 2011).

In the top panel of Fig 7, the distribution of maximum amplitude for δ Sct stars with $K_p < 12.5$ mag is shown. As might be expected, the number of stars increases as the amplitude decreases. If we assume that the non-pulsating stars are actually pulsating below the detection level, they should also be included in this distribution. They must then be added to the number in the bin with the lowest amplitude

covering amplitudes between 0 and 10 ppm. If that is done, there is a discontinuous jump in the amplitude distribution, as seen in the bottom panel of Fig. 7, which does not appear to be physical.

The only way of avoiding this strange behaviour in the amplitude distribution is to assume that the non-pulsating stars belong to a different population and should not be included in the amplitude distribution of the pulsating stars. In other words, the simplest explanation is that the non-pulsating stars are not pulsating below the detection limit and do not pulsate at all. It can be concluded that the δ Sct instability strip is not pure. As already mentioned, this poses a serious problem. We seem to have an incomplete understanding of the outer layers of A stars.

The conclusion here differs from that of Murphy et al. (2015). From a study of only 54 stars, they found that all stars within the δ Sct instability strip pulsate. Guzik et al. (2014) found that most stars pulsate, but a few constant stars remain. It could be argued that most of the constant stars are outside the instability strip due to errors in the effective temperature. The typical error in T_{eff} is about 200–300 K, while the width of the instability strip is about 3000 K. To move a star in the middle of the instability strip to the edges of the strip requires that T_{eff} be in error by about 5 standard deviations (a probability less than 10^{-5}). Of course, the probability will be higher if the star is closer to the edge of the instability strip, but it means that the probability that all 1781 non-pulsating stars are outside the instability strip is the product of the individual probabilities which is essentially zero. Furthermore, one has to assume that (for some unknown reason) the values of T_{eff} for δ Sct stars are much more accurate, otherwise many of these δ Sct stars would also be moved out of the instability region.

For these reasons it is a certainty that non-pulsating stars exist in the instability region unless the discontinuity in the amplitude distribution can be understood in some other way.

8 HIGH-AMPLITUDE δ SCT STARS

The high-amplitude δ Sct stars (HADS) are a well-known group characterized by high photometric amplitude (generally higher than 0.3 mag) and fairly simple frequency spectra, but with many combination frequencies. None of the stars in the *Kepler* field attain such a large amplitude, but several are known in the general field. They have been assumed to be transition objects between Cepheids and δ Sct stars - in fact they were originally called “dwarf Cepheids”.

It is interesting to locate the field HADS in the H-R diagram to determine their evolutionary status. Using the catalogue of Rodriguez et al. (2000), all stars with amplitudes exceeding 0.3 mag were selected. Gaia DR2 parallaxes were obtained for those stars which have effective temperatures from Apsis-Priam (Bailer-Jones et al. 2013). These effective temperatures are available in the Gaia DR2 catalogue. The interstellar absorption was estimated using the 3D map of Gontcharov (2017). Results are shown in Table 4. Some of the HADS appear to be evolved stars belonging to Population II on the basis of their high proper motions and low metallicities. These are called SX Phe variables.

Fig. 8 shows the HADS in the H-R diagram. They ap-

Table 4. List of HADS stars with know effective temperatures. Column two is the type of star. The light amplitude is from the catalogue of [Rodríguez et al. \(2000\)](#). The parallax is from Gaia DR2 and the interstellar absorption, A_V mag, is from the table in [Gontcharov \(2017\)](#). The effective temperature is from the Apsis-Prism compilation in the Gaia DR2 catalogue and has a typical error of about 250 K. The last column is the luminosity with typical error of 0.04 dex.

Star	Type	Amp mag	Plx mas	A_V mag	T_{eff} K	$\log \frac{L}{L_{\odot}}$
XX Cyg	SXPHE	0.80	0.84 ± 0.04	0.55	6982	1.50
KZ Hya	SXPHE	0.80	2.98 ± 0.10	0.27	7239	1.07
CY Aqr	SXPHE	0.71	2.34 ± 0.05	0.39	7271	0.93
AI Vel	DSCT	0.67	9.86 ± 0.03	0.31	6944	1.43
RS Gru	DSCT	0.56	4.03 ± 0.05	0.24	7226	1.49
DY Peg	SXPHE	0.54	2.45 ± 0.07	0.39	7646	1.14
GP And	DSCT	0.52	1.94 ± 0.15	0.37	7718	1.14
DY Her	DSCT	0.51	1.39 ± 0.04	0.36	6920	1.58
SZ Lyn	DSCT	0.51	2.49 ± 0.07	0.22	7799	1.41
EH Lib	DSCT	0.50	2.72 ± 0.05	0.37	7011	1.23
VZ Cnc	DSCT	0.50	4.43 ± 0.05	0.22	6812	1.65
V4425 Sgr	SXPHE	0.49	2.22 ± 0.05	0.54	7029	1.59
BS Aqr	DSCT	0.44	1.98 ± 0.06	0.27	7009	1.69
AE UMa	SXPHE	0.44	1.28 ± 0.07	0.24	7825	1.25
CW Ser	DSCT	0.43	0.53 ± 0.04	0.61	7271	1.96
YZ Boo	DSCT	0.42	1.68 ± 0.03	0.29	7365	1.36
VX Hya	DSCT	0.40	0.99 ± 0.04	0.38	6694	1.82
BE Lyn	DSCT	0.39	3.86 ± 0.05	0.07	7806	1.23
SS Psc	DSCT	0.39	0.82 ± 0.12	0.41	7286	1.88
ZZ Mic	DSCT	0.35	2.96 ± 0.05	0.26	7757	1.28
RY Lep	DSCT	0.35	2.46 ± 0.05	0.21	7122	1.90
V0567 Oph	DSCT	0.33	1.45 ± 0.04	1.02	5727	1.59
DE Lac	DSCT	0.32	1.28 ± 0.04	0.59	6109	1.88
V1719 Cyg	DSCT	0.31	2.52 ± 0.03	0.39	6531	2.09
AD CMi	DSCT	0.30	2.18 ± 0.04	0.24	7129	1.60

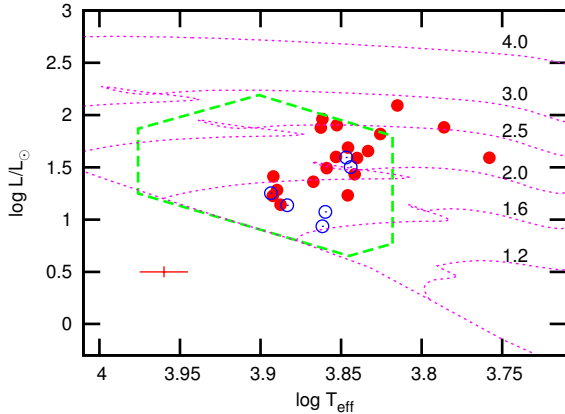


Figure 8. Location of the HADS in the H-R diagram. The filled circles are HADS of the δ Sct type and the open circles are SX Phe stars. The δ Sct box, the ZAMS and evolutionary tracks (masses labeled) from [Bertelli et al. \(2008\)](#) are shown.

pear to lie in the middle of the instability strip except for V0567 Oph which has a very low effective temperature. The SX Phe group also lie well within the instability box. If HADS were transition objects between δ Sct and Cepheids, one would expect all of them to have high luminosities, intermediate between the two groups of variables. However, most HADS appear to be normal δ Sct stars.

Fig. 9 shows how the typical maximum amplitude in δ Sct stars varies within the instability strip. Largest ampli-

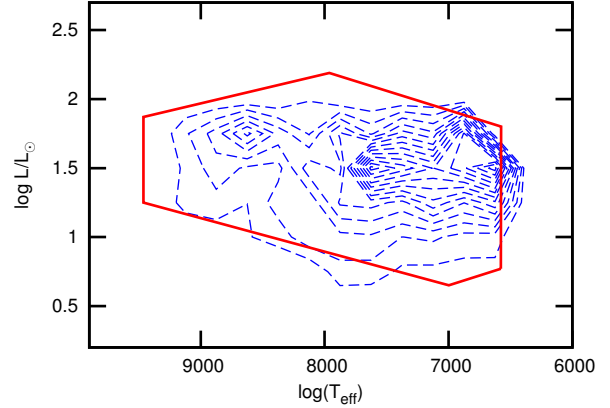


Figure 9. Contours showing maximum pulsation amplitudes of δ Sct stars in the H-R diagram with polygonal region of instability. The contours show amplitudes from 500 to 7000 ppm.

tudes tend to occur around $T_{\text{eff}} \approx 7000$ K among the more luminous cool δ Sct stars. The mean effective temperature of the HADS is 7200 ± 200 which suggests that the high amplitudes in HADS are in line with what might be expected in normal δ Sct stars. The reason why the amplitude is so much larger in HADS compared to normal δ Sct stars can only be answered by nonlinear, nonradial pulsation models which do not yet exist.

9 CONCLUSIONS

Using the full four-year light curves and periodograms of stars in the *Kepler* field, all stars with *Kepler* magnitude $K_p < 12.5$ mag, as well as many more fainter stars, were classified according to variability type. A catalog of δ Sct and γ Dor stars with Gaia DR2 parallaxes is presented. From these data, luminosities, $\log L/L_{\odot}$, with a standard deviation of 0.04 dex. By contrast, previous luminosity estimates based on multicolour photometry have typical errors of 0.4 dex.

The most surprising result is that the γ Dor variables do not occupy a separate instability strip, but lie entirely within the δ Sct instability region. There are, in fact, more δ Sct stars inside the γ Dor instability region than γ Dor stars. No two classes of pulsating star are known to share the same instability region. This must be the case if the driving and damping mechanisms differ, as they do in the conventional explanation for the two classes: the opacity κ mechanism for δ Sct stars and the convective blocking mechanism for γ Dor stars.

It seems that the frequencies in γ Dor stars may be just an effect of mode selection rather than reflecting different driving and damping mechanisms. The presence of a large variety of light curves among the γ Dor stars, classified here as GDORA, GDORS and GDORM is probably an indication of the sensitivity of mode selection to the conditions in the outer layers of the star. The GDORA type, for example, shows extreme non-linear effects. Why such nonlinearity exists only in a subset of these stars is not known. This effect is not seen in δ Sct stars, but it might be masked by the presence of other frequencies of higher amplitudes. The sug-

gestion by Xiong et al. (2016) that γ Dor stars should not be seen as a separate class has great merit. Nevertheless, the distinction is still a useful one for classification purposes.

Our understanding of stellar pulsation has evolved quite considerably over the last few decades. It is now recognized that multiple driving and damping mechanisms occur in the same star. The most important recent works in this respect are that of Xiong et al. (2015) and Xiong et al. (2016) where it is demonstrated that the interplay of different processes can account for the instability at low frequencies seen in practically all δ Sct stars. In fact, inspection of the *Kepler* light curves shows that low frequencies are present in at least 98 percent of δ Sct stars.

The work of Xiong et al. (2016) offers a very attractive explanation for the low frequencies in δ Sct stars. Unfortunately, the predicted red and blue edges from Xiong et al. (2016) do not agree with the limits of the instability regions determined in this paper. It is also not clear whether an explanation for the co-existence of γ Dor, δ Sct and non-pulsating stars can be found by tuning available free parameters in the theory. Nevertheless, this work shows great promise for a better understanding of these stars.

Another well-known group among the δ Sct stars are the HADS. In this paper it is shown that most HADS are normal δ Sct stars.

The data analyzed in this paper indicates that the majority of stars within the δ Sct instability region do not pulsate. If it is assumed that these stars actually pulsate below the detectable level, then they should be included in the calculation of the distribution of maximum amplitude. In that case, the very large number of apparently non-pulsating stars introduces a nonphysical discontinuity in the distribution of maximum amplitudes. This suggests that these stars do not pulsate. This introduces yet another unresolved issue because a reason needs to be found for the high damping of pulsations in the majority of stars in the instability region.

It appears that one or more unknown damping and driving processes are operating in the outer layers, rendering the pulsation amplitudes and mode selection very sensitive to conditions in these layers. These problems are perhaps not too surprising in view of the fact that starspots are present in most A stars (Balona 2017). None of the current models of A stars provide a possible explanation for the presence of starspots. The problems discussed here add to the need for a revision in the current view of A star atmospheres.

ACKNOWLEDGMENTS

LAB wishes to thank the National Research Foundation of South Africa for financial support. This work has made use of data from the European Space Agency (ESA) mission Gaia (<https://www.cosmos.esa.int/gaia>), processed by the Gaia Data Processing and Analysis Consortium (DPAC, <https://www.cosmos.esa.int/web/gaia/dpac/consortium>). Funding for the DPAC has been provided by national institutions, in particular the institutions participating in the Gaia Multilateral Agreement. This paper includes data collected by the Kepler mission. Funding for the Kepler mission is provided by the NASA Science Mission directorate.

REFERENCES

- Bailer-Jones C. A. L., Andrae R., Arcay B., Astraatmadja T., Bellas-Velidis I., Berihuete A., Bijaoui A., Carrión C., Dafonte C., Damerdjy Y., Dapergolas A., de Laverny P., Delchambre L., Drazinos P., Drimmel R., Frémat Y., Fustes D., García-Torres M., Guédé C., Heiter U., Janotto A.-M., Karampelas A., Kim D.-W., Knude J., Kolka I., Kontizas E., Kontizas M., Korn A. J., Lanzafame A. C., Lebreton Y., Lindstrøm H., Liu C., Livanou E., Lobel A., Manteiga M., Martayan C., Ordenovic C., Pichon B., Recio-Blanco A., Rocca-Volmerange B., Sarro L. M., Smith K., Sordo R., Soubiran C., Surdej J., Thévenin F., Tsalmantza P., Vallenari A., Zorec J., 2013, *A&A*, 559, A74
- Balona L. A., 2014, *MNRAS*, 437, 1476
- , 2017, *MNRAS*, 467, 1830
- , 2018, *MNRAS*, 476, 4840
- Balona L. A., Abedigamba O. P., 2016, *MNRAS*, 461, 497
- Balona L. A., Daszyńska-Daszkiewicz J., Pamyatnykh A. A., 2015, *MNRAS*, 452, 3073
- Balona L. A., Dziembowski W. A., 2011, *MNRAS*, 417, 591
- Balona L. A., Engelbrecht C. A., Joshi Y. C., Joshi S., Sharma K., Semenko E., Pandey G., Chakradhari N. K., Mkrtichian D., Hema B. P., Nemec J. M., 2016, *MNRAS*, 460, 1318
- Balona L. A., Guzik J. A., Uytterhoeven K., Smith J. C., Tenenbaum P., Twicken J. D., 2011, *MNRAS*, 415, 3531
- Bertelli G., Girardi L., Marigo P., Nasi E., 2008, *A&A*, 484, 815
- Brown T. M., Latham D. W., Everett M. E., Esquerdo G. A., 2011, *AJ*, 142, 112
- Castelli F., Kurucz R. L., 2003, in *IAU Symposium*, Vol. 210, *Modelling of Stellar Atmospheres*, Piskunov N., Weiss W. W., Gray D. F., eds., p. A20
- Dupret M., Grigahcène A., Garrido R., Gabriel M., Scuflaire R., 2005a, *A&A*, 435, 927
- Dupret M.-A., Grigahcène A., Garrido R., De Ridder J., Scuflaire R., Gabriel M., 2005b, *MNRAS*, 361, 476
- Gaia Collaboration, Brown A. G. A., Vallenari A., Prusti T., de Bruijne J. H. J., Babusiaux C., Bailer-Jones C. A. L., 2018, *ArXiv e-prints*
- Gaia Collaboration, Prusti T., de Bruijne J. H. J., Brown A. G. A., Vallenari A., Babusiaux C., Bailer-Jones C. A. L., Bastian U., Biermann M., Evans D. W., et al., 2016, *A&A*, 595, A1
- Gontcharov G. A., 2017, *Astronomy Letters*, 43, 472
- Grigahcène A., Antoci V., Balona L., Catanzaro G., Daszyńska-Daszkiewicz J., Guzik J. A., Handler G., Houdek G., Kurtz D. W., Marconi M., Monteiro M. J. P. F. G., Moya A., Ripepi V., Suárez J., Uytterhoeven K., Borucki W. J., Brown T. M., Christensen-Dalsgaard J., Gilliland R. L., Jenkins J. M., Kjeldsen H., Koch D., Bernabei S., Bradley P., Breger M., Di Criscienzo M., Dupret M., García R. A., García Hernández A., Jackiewicz J., Kaiser A., Lehmann H., Martín-Ruiz S., Mathias P., Molenda-Žakowicz J., Nemec J. M., Nuspi J., Páparó M., Roth M., Szabó R., Suran M. D., Ventura R., 2010, *ApJ*, 713, L192
- Guzik J. A., Bradley P. A., Jackiewicz J., Uytterhoeven K., Kinnemuchi K., 2014, in *IAU Symposium*, Vol. 301, *Precision Asteroseismology*, Guzik J. A., Chaplin W. J., Handler G., Pigulski A., eds., pp. 63–66
- Guzik J. A., Kaye A. B., Bradley P. A., Cox A. N., Neuforge C., 2000, *ApJ*, 542, L57
- Handler G., Balona L. A., Shobbrook R. R., Koen C., Bruch A., Romero-Colmenero E., Pamyatnykh A. A., Willems B., Eyer L., James D. J., Maas T., 2002, *MNRAS*, 333, 262
- Houdek G., 2000, in *Astronomical Society of the Pacific Conference Series*, Vol. 210, *Delta Scuti and Related Stars*, M. Breger & M. Montgomery, ed., pp. 454–+
- Houdek G., Dupret M.-A., 2015, *Living Reviews in Solar Physics*,

- Huber D., Silva Aguirre V., Matthews J. M., Pinsonneault M. H., Gaidos E., García R. A., Hekker S., Mathur S., Mosser B., Torres G., Bastien F. A., Basu S., Bedding T. R., Chaplin W. J., Demory B.-O., Fleming S. W., Guo Z., Mann A. W., Rowe J. F., Serenelli A. M., Smith M. A., Stello D., 2014, *ApJS*, 211, 2
- Mowlavi N., Barblan F., Saesen S., Eyer L., 2013, *A&A*, 554, A108
- Murphy S. J., Bedding T. R., Niemczura E., Kurtz D. W., Smalley B., 2015, *MNRAS*, 447, 3948
- Papaloizou J., Pringle J. E., 1978, *MNRAS*, 182, 423
- Pinsonneault M. H., An D., Molenda-Żakowicz J., Chaplin W. J., Metcalfe T. S., Bruntt H., 2012, *ApJS*, 199, 30
- Qian S.-B., Li L.-J., He J.-J., Zhang J., Zhu L.-Y., Han Z.-T., 2018, *MNRAS*, 475, 478
- Rodriguez E., Lopez-Gonzalez M. J., Lopez de Coca P., 2000, *VizieR Online Data Catalog*, 414
- Saio H., Kurtz D. W., Murphy S. J., Antoci V. L., Lee U., 2018, *MNRAS*, 474, 2774
- Smith J. C., Stumpe M. C., Van Cleve J. E., Jenkins J. M., Barclay T. S., Fanelli M. N., Girouard F. R., Kolodziejczak J. J., McCauliff S. D., Morris R. L., Twicken J. D., 2012, *PASP*, 124, 1000
- Stumpe M. C., Smith J. C., Van Cleve J. E., Twicken J. D., Barclay T. S., Fanelli M. N., Girouard F. R., Jenkins J. M., Kolodziejczak J. J., McCauliff S. D., Morris R. L., 2012, *PASP*, 124, 985
- Uytterhoeven K., Moya A., Grigahcène A., Guzik J. A., Gutiérrez-Soto J., Smalley B., Handler G., Balona L. A., Niemczura E., Fox Machado L., Benatti S., Chapellier E., Tkachenko A., Szabó R., Suárez J. C., Ripepi V., Pascual J., Mathias P., Martín-Ruiz S., Lehmann H., Jackiewicz J., Hekker S., Gruberbauer M., García R. A., Dumusque X., Díaz-Fraile D., Bradley P., Antoci V., Roth M., Leroy B., Murphy S. J., De Cat P., Cuypers J., Kjeldsen H., Christensen-Dalsgaard J., Breger M., Pigulski A., Kiss L. L., Still M., Thompson S. E., van Cleve J., 2011, *A&A*, 534, A125
- Xiong D.-R., 1989, *A&A*, 209, 126
- Xiong D. R., Cheng Q. L., Deng L., 1998, *ApJ*, 500, 449
- Xiong D. R., Deng L., Zhang C., 2015, *MNRAS*, 451, 3354
- Xiong D. R., Deng L., Zhang C., Wang K., 2016, *MNRAS*, 457, 3163